Long-Term Neuroprotective Effects of NT-4–Engineered Mesenchymal Stem Cells Injected Intravitreally in a Mouse Model of Acute Retinal Injury

Anna Machalińska,[1] Miłosz Kawa,[2] Ewa Pius-Sadowska,[2] Jacek Stępniewski,[3] Witold Nowak,[3] Dorota Rogińska,[2] Katarzyna Kaczyńska,[2] Bartłomiej Baumert,[2] Barbara Wiszniewska,[1] Alicja Józkowicz,[3] Józef Dulak,[3] and Bogusław Machaliński[2]

[1]Department of Histology and Embryology, Pomeranian Medical University, Szczecin, Poland
[2]Department of General Pathology, Pomeranian Medical University, Szczecin, Poland
[3]Department of Medical Biotechnology, Faculty of Biochemistry, Biophysics and Biotechnology, Krakow, Poland

Correspondence: Bogusław Machaliński, Department of General Pathology, Pomeranian Medical University, Powstancow Wlkp. 72, 70-111 Szczecin, Poland; machalin@pum.edu.pl.
Anna Machalińska, Department of Histology and Embryology, Pomeranian Medical University Powstancow Wlkp. 72, 70-111 Szczecin, Poland; annam@pum.edu.pl.

AM and MK contributed equally to the work presented here and should therefore be regarded as equivalent authors.

Submitted: April 13, 2013
Accepted: November 12, 2013

Citation: Machalińska A, Kawa M, Pius-Sadowska E, et al. Long-term neuroprotective effects of NT-4–engineered mesenchymal stem cells injected intravitreally in a mouse model of acute retinal injury. *Invest Ophthalmol Vis Sci*. XXXX;XX:XXX–XXX. DOI: 10.1167/iovs.13-12221

Purpose. Retinal degenerative diseases targeting the RPE and adjacent photoreceptors affect millions of people worldwide. The field of stem cell– and gene-based therapy holds great potential for the treatment of such diseases. The present study sought to graft genetically engineered mesenchymal stem cells (MSCs) that continuously produce neurotrophin-4 (NT-4) into the murine eye after the onset of acute retinal injury.

Methods. C57BL/6 mice were subjected to acute retinal damage using a low dose of sodium iodate (20 mg/kg of body weight), followed by intravitreal injection of lentivirally modified MSC-NT-4 into the right eye. At 3 months after the MSC transplantation grafted cell survival, retinal function and gene expression were analyzed.

Results. Immunofluorescence analysis confirmed that transplanted MSCs survived for at least 3 months after intravitreal injection and preferentially migrated toward sites of injury within the retina. MSC-NT-4 actively produced NT-4 in the injured retina and significantly protected damaged retinal cells, as evaluated by ERG and optical coherence tomography (OCT). Of importance, the long-term therapy with MSC-NT-4 was also associated with induction of prosurvival signaling, considerable overexpression of some subsets of transcripts, including several members of the crystallin β-γ superfamily (*Cryba4*, *Crybb3*, *Cryba2*, *Crybb1*, *Crybb2*, *Cryba1*, and *Crygc*) and significant upregulation of biological processes associated with visual perception, sensory perception of light stimulus, eye development, sensory organ development, and system development.

Conclusions. Transplantation of genetically modified MSCs that produce neurotrophic growth factors may represent a useful strategy for treatment of different forms of retinopathies in the future.

Keywords: electroretinography, gene expression, gene therapy, MSCs, neurotrophin-4, retinal injury, sodium iodate

Inherited or acquired retinal degeneration involving the RPE and photoreceptors is a major cause of blindness throughout the world. Therefore, there is an enormous need to develop therapeutic strategies to protect retinal function and structure in these patients. Although the underlying causes of retinal degeneration have not been clearly elucidated, many factors that may contribute to retinal neurodegeneration have been identified, including decreased production of vital trophic factors, increased oxidative stress, and reactive changes in retinal cells owing to metabolic stress and to activation of inflammatory responses. Several approaches have been undertaken to slow and eventually stop the degeneration process, but their therapeutic effects are transient and very limited.[1–3] Neurotrophins (NTs) are a family of growth factors including neural growth factor (NGF), brain-derived growth factor (BDNF), neurotrophin-3 (NT-3), and neurotrophin-4/5 (NT-4/5) in mammals as well as NT-6 and -7 in fish.[4] It is well known that the major role of NTs is to promote neuronal survival.[5] However, in recent decades, their functions have been extended to also include cell migration and cell proliferation.[6] Neurotrophins mediate many of their effects via receptor tyrosine kinases (TrkA, TrkB, and TrkC); BDNF and NT-4 have been shown to induce signaling primarily through the same receptor, TrkB.[7] TrkB stimulation results in the activation of several kinases that belong to intracellular signaling cascades, including the phosphatidylinositol-3-OH kinase (PI3K)/Akt pathway, the Ras/extracellular signal-regulated kinase (ERK) pathway, and phospholipase C-γ1 (PLC-γ1).[8] Most important, Akt is a serine/threonine (ser/thr) protein kinase that promotes cell survival through the activation of PI3-K. This signaling molecule is activated by a number of growth factors and cytokines and serves as a multifunctional regulator of cell biology and protein synthesis.[9] Akt is also thought to be one of the molecules that prevents apoptosis.[10,11] Similarly, upon activation, ERK1/2, which represents the crucial component

of the mitogen-activated protein kinase (MAPK) complex, can phosphorylate a variety of intracellular targets, including transcription factors, membrane transporters, cytoskeletal elements, and other protein kinases. This process leads to cell survival, differentiation, migration, and development.[12]

The expression of NTs and their receptors has been studied extensively in the central nervous system (CNS), including the visual system,[13–15] and neuronal protection and enhancement of neurite outgrowth/axonal regeneration mediated by BDNF and NT-4/5 is well documented.[16] More important, these molecules are also locally produced in the retina,[17–19] and it is postulated that these NTs may contribute to different aspects of differentiation, proliferation, neuroprotection, and survival of photoreceptors and other targets in the retina.[20–23] A recent study reported that NT-4 is upregulated in the Müller cells of patients with proliferative vitreoretinopathy, which may serve as a mechanism for neuroprotection against retinal injury.[24] Similarly, several reports have indicated that Müller glia express the high-affinity TrkB[25] and low-affinity p75 NT receptors[26] and thus might be influenced by BDNF and NT-4 treatment. Of interest, exogenously applied BDNF has been shown to increase the number of neuronal progenies.[27] Although intravitreal supplementation of exogenous BDNF and NT-4 has been reported to enhance the survival of injured adult retinal cells such as RGCs,[28–30] this protective effect is only transient and fails to prevent eventual retinal cell death.[31] Given that intraocular injection of NTs was only shown to temporarily rescue injured retinas, we examined the potential neuroprotective effect following prolonged NT-4 application via combined cellular and gene therapy.

Mesenchymal stem cells (MSCs) are an attractive vehicle for combined cellular and gene therapies. To date, MSCs have been extensively tested and proven effective in preclinical studies of many disorders, including neurodegenerative diseases.[32] Of importance, MSCs have also shown the potential to be neuroprotective when used for therapy in certain animal models of retinal degeneration[33–35] and glaucoma.[36] From a clinical perspective, MSCs have been successfully harvested from bone marrow and fat tissue, with minimal discomfort for the patient,[37] thus providing an excellent source of cells for combined cellular and gene therapies in humans.

Several strategies are currently being developed for introducing growth factor genes into MSCs. To date, the rates of transfection efficiency into these cells using plasmid, retroviral, and adenoviral vectors were shown to be 1%, 18% to 65%, and 20%, respectively.[38–40] It was also recently shown that the transduction efficiency of lentiviral vectors into MSCs was much greater than that observed with other vectors routinely used in gene therapy.[41] Thus, lentivirus-based engineering of bone marrow–derived MSCs to continuously produce neurotrophic growth factors has been proposed as an attractive approach for the long-term delivery of neuroprotective substances such as NTs to the injured CNS in various animal models.[42–44]

No studies have specifically analyzed the effect of NT-4 on either photoreceptors or RPE cells after chemically induced acute retinal injury. In this study, we demonstrate that genetically modified MSCs transduced to express NT-4 (MSCs-NT-4) using lentiviral vectors were capable of long-term survival (up to 3 months) in eyes after intravitreal transplantation and the continuous delivery of NT-4, which resulted in significant improvements in the functional parameters observed by ERG. We also sought to characterize the molecular mechanisms underlying the long-term protective effect of NT-4 and the signaling pathways supporting the survival of retinal cells.

Materials and Methods

Production of Recombinant Lentivirus Carrying the Human NT-4 Gene

The lentiviral vector containing human neurotrophin-4 (Lv-UbC-NT-4) was constructed based on the pFUGW plasmid from Addgene (#14883),[45] which enables the expression of transgenes under the human ubiquitin C promoter (UbC). The NT-4 coding sequence (Gene Bank NM_006179.4) was obtained from human primary keratinocytes by PCR with specific primers flanked with BamHI and EcoRI recognition sites. The amplified NT-4 sequence was gel-purified, digested, and inserted into the pFUGW plasmid backbone, from which the green fluorescent protein (GFP) sequence was removed with the same pair of restriction endonucleases. The schematic constructions of both plasmids used in this study are presented in Figure 1A. The pFUW-NT-4 plasmid DNA was identified with restriction endonucleases (EcoRI and BamHI). The correct band for NT-4 (666 bp) was observed under UV light in agarose gel (Fig. 1B). To produce lentiviral vectors, 293T packaging cells were transfected with either pFUW-NT-4 or pFUGW (for production of control Lv-UbC-GFP vectors) as well as psPAX2 and pMD2.G plasmids using polyethyleneimine (Polysciences, Inc., Warrington, PA). Vector-containing medium was collected 48 hours after transfection and filtered through 0.45-μm filters.

Isolation of MSCs

Bone marrow MSCs were isolated from the femurs and tibias of 4- to 6-week-old C57BL/6 mice, according to a modification of the protocol described by Zhu et al.[46] The epiphyses of the femurs and tibias were removed, and bones were dissected into small fragments that were digested with 1 mg/mL collagenase type II (Gibco, Carlsbad, CA) in α-MEM medium (Lonza, Basel, Switzerland) supplemented with 10% fetal bovine serum (FBS; Gibco), 100 U/mL penicillin, and 100 μg/mL streptomycin (Sigma-Aldrich, St. Louis, MO) for 1.5 hours in a shaking incubator at 37°C. Then, released cells were washed with PBS and seeded onto 100-mm cell culture dishes in 8 mL α-MEM. The medium was changed after 72 hours and every 3 to 4 days thereafter. Cells were harvested with Accutase (10-minute treatment in a 37°C incubator; PAA, Pasching, Austria) when 100% confluence was reached. A representative photomicrograph of cultured MSCs is shown in Figure 1C.

Identification of MSCs

After four to five passages, cells were detached with Accutase, immunophenotyped with anti-CD45-V450 (BD Pharmingen, Franklin Lakes, NJ), anti-CD31-FITC (BD Pharmingen), anti-Ly-6A/E(Sca-1)-PE (BioLegend, San Diego, CA), anti-CD90.2-APC (BioLegend), and anti-CD105-PE-Cy7 (BioLegend) antibodies using a BD LSR II flow cytometer (Becton Dickinson Biosciences, San Jose, CA). Cultured plastic-adherent bone marrow–derived cells were then depleted of the contaminating $CD45^+$ hematopoietic cells with anti-mouse CD45 MicroBeads (Miltenyi Biotec, Bergisch Gladbach, Germany) using the AutoMACS platform (Miltenyi Biotec). The data were analyzed with CellQuest Software (Becton ~~Dickinson~~). The representative phenotypic analysis of cultured murine MSCs by fluorescence-activated cell sorting (FACS) is presented in Figure 1D.

Lentiviral Transduction of Murine MSCs

MSCs were genetically engineered to produce and secrete the NT-4 neurotrophic factor using a lentiviral vector. Briefly, MSCs were plated in 12-well plates (BD Pharmingen) at a density of

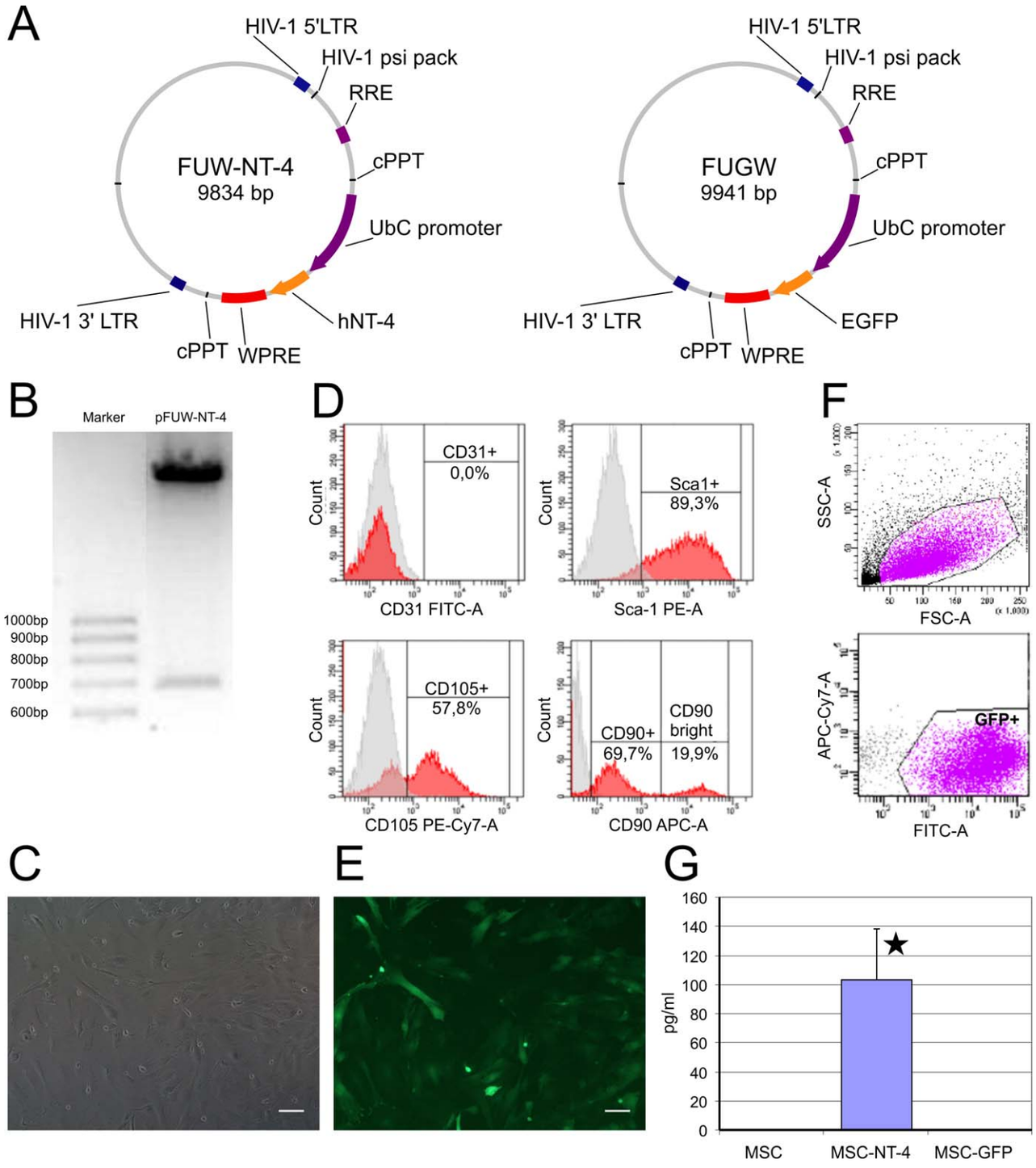

Figure 1. Characterization of isolated murine MSCs and their subsequent lentiviral transduction efficiency. (**A**) Schematic maps of the plasmids utilized to produce lentiviral vectors for infection of mouse MSCs. The Lv-UbC-NT-4 lentivirus construct contained human NT-4 coding sequence, whereas Lv-UbC-GFP vector contained the GFP coding sequence. (**B**) The pFUW–NT-4 plasmid DNA encoding NT-4 was identified with restriction endonucleases (EcoRI and BamHI). The correct band for NT-4 (666 bp) was observed under UV light in agarose gel. (**C**) Flow cytometry histograms of murine MSCs demonstrating the typical expression pattern of surface antigens (Sca-1, CD105, and CD90, and negative for CD31). (**D**) The GFP-positive MSCs were analyzed by FACS after collecting 10.000 events. The cells were approximately 95% positive for GFP. (**E**, **F**) Photomicrographs of cultured MSCs. *Scale bar*: 100 μm. Phase contrast images in (**E**) show the characteristic spindle shape of adherent MSCs. (**F**) Fluorescent images in (**E**) show that infected GFP-positive MSCs (third day post infection with Lv-UbC-GFP) had a morphology identical to that of nontransduced control MSCs. (**G**) Quantitative analysis of NT-4 levels from MSC-NT-4 cultures in vitro. Noninfected MSCs and Lv-UbC-GFP–infected MSCs did not produce NT-4 protein at detectable levels.

Investigative Ophthalmology & Visual Science

10^5 cells per well in 500 μL α-MEM (10% FBS, antibiotics) and allowed to adhere for 12 hours. Then, the α-MEM growth medium was supplemented with 4 μg/well of polybrene (Sigma-Aldrich, St. Louis, MO). Next, the Lv-UbC-NT-4 vector (which was decanted from the 293T-cell culture after transfection) was added to the prepared MCSs for a final volume of 1000 μL. In parallel, a population of control MSCs was engineered with only the Lv-UbC-GFP in the same ratio as the NT-4–engineered MSCs to match the viral titer. Viral particles were removed from the MSC cultures after 72 hours of exposure by exchange of the culture medium. Next, both engineered MSC populations (MSC-NT-4 and MSC-GFP) were maintained as previously described. MSC-GFP cultures were examined for GFP fluorescence at 72 hours after initial viral transduction and then passaged after 4 days (Fig. 1E). Similarly, an ELISA was employed at 72 hours to measure the amount of NT-4 in the medium from MSC-NT-4 cultures.

Flow Cytometry of GFP-Positive MSCs

Uninfected MSCs and MSC-GFP were harvested from tissue culture flasks at day 3 post infection and divided into aliquots of 5×10^4 cells. Suspensions were rinsed with sterile PBS, centrifuged at 300*g* for 8 minutes, and then rinsed briefly with propidium iodide solution (Sigma-Aldrich) to label dead cells. Next, cells were centrifuged at 300*g* for 8 minutes, resuspended in 1-mL PBS, and then analyzed by FACS (LSRII instrument; Becton Dickinson Biosciences) using CellQuest Software (Becton Dickinson Biosciences).

ELISA

Levels of NT-4 in the culture medium from MSC-NT-4 cultures were measured using the commercially available high-sensitivity ELISA Quantikine human immunoassay kit (R&D Systems, McKinley Place, MN) according to the manufacturer's protocol. The absorbance was read at 450 nm using an ELX 808 IU automated Microplate Reader (Bio-Tek Instruments, Inc., Winooski, VT). The results were analyzed using a quadratic log–log curve fit.

Animals and Experimental Procedures

Pathogen-free 8- to 12-month-old mature male C57BL mice (Polish Academy of Sciences, Wroclaw, Poland) weighing 27 to 29 g were used in the experiment. Mice were anesthetized, and sodium iodate (Sigma-Aldrich) in PBS at a dose of 20 mg/kg body weight was injected intravenously into the retro-orbital sinus. In the 24 hours post injury, 1 μL of PBS containing MSCs expressing NT-4 (MSC-NT-4) or GFP (MSC-GFP) (1×10^5 cells/μL) was injected intravitreally into the right eye using a 30-gauge needle attached to a Hamilton syringe (Hamilton Company, Reno, NV). The left eye, which was injected with uninfected MSCs, served as the control. Prior to the procedure, the mice were anesthetized with an intraperitoneal injection of ketamine (40 mg/kg) and xylazine (4 mg/kg), and their pupils were dilated with eye drops containing 0.5% tropicamide and 2.5% phenylephrine hydrochloride. Additionally, the ocular surface was anesthetized with a topical application of 0.5% proparacaine hydrochloride eye drops. Mouse retinas were monitored for functional recovery by ERG, and mice were killed 3 months after the intravitreal MSC injection. All animal procedures were performed according to the regulations in the ARVO Statement for the Use of Animals in Ophthalmic and Vision Research and were approved by the local ethics committee.

Histologic and Immunofluorescence Analysis

For cross-sections, the eyes were embedded in paraffin, cut into 5-μm-thick sections, and routinely stained with hematoxylin and eosin (H&E; Sigma-Aldrich). For immunohistochemical analysis, the sections were deparaffinized in xylene (2×15 minutes) followed by hydration in decreasing ethanol concentration solutions (100%, 95%, 85%, 70%, and 50%) and antigen retrieval (20 minutes of boiling in citrate buffer, pH 6.0). After blocking in 10% normal serum (goat or donkey, depending on the host species of the secondary antibody), the sections were incubated with the primary antibodies (abs) in PBS complemented with 1% BSA: chicken anti-GFP antibody (1:1000; Abcam, Cambridge, UK), rabbit anti-opsin red/green (1:100; Merck KGaA, Darmstadt, Germany), rabbit anti-opsin blue (1:100; Merck KGaA), sheep anti-TrkB (1:50; Novus Biologicals, Littleton, CO), respectively, at 4°C overnight. Next, incubation with secondary abs for 1 hour at room temperature in the dark was performed: goat anti-chicken-Alexa Fluor-488 antibody (1:100; Life Technologies, Paisley, UK), goat anti-rabbit-TR (1:100; Vector Laboratories, Burlingame, CA), or donkey anti-sheep-Alexa Fluor-647 (1:50; Life Technologies). For co-expression with rhodopsin, slides were additionally incubated with the primary mouse anti-rhodopsin ab (1:500; Abcam) followed by the incubation with the secondary ab: chicken anti-mouse-Alexa Fluor-488 (1:100; Life Technologies). For co-expression with proliferating cell nuclear antigen (PCNA), slides were additionally incubated with the primary goat anti-PCNA ab (1:100; Santa Cruz Biotechnology, Santa Cruz, CA) followed by the incubation with the secondary ab: donkey anti-goat-Alexa Fluor-647 (1:100; Life Technologies). Upon termination, all sections were then counterstained with DAPI solution (Thermo Scientific, Pittsburgh, PA), mounted, and subjected to microscopic analysis using an LSM700 confocal system (Carl Zeiss, Jena, Germany). At least five eye-tissue sections, derived from different parts of retinas of five independent animals/time point of the experiment, were analyzed.

Western Blot Analysis

For Western blot analysis, retinas were homogenized in M-Per lysing buffer (Pierce, Rockford, IL) containing protease and phosphatase inhibitors (10 μg/mL leupeptin, 10 μg/mL aprotinin, 1 μg/mL pepstatin A, 1 mM sodium fluoride, and 2 mM Na_3VO_4; Sigma-Aldrich), and proteins were extracted using the PARIS Kit (Life Technologies). Briefly, the mixture was centrifuged, supernatants were isolated, and protein concentrations were determined using the Bradford protein assay (Sigma-Aldrich). Equal amounts of protein (20 μg/well) were loaded and separated by 4% to 20% SDS-PAGE (mini-PROTEAN II electrophoresis system; Bio-Rad, Hercules, CA) and then transferred to a 0.2-μm polyvinylidene fluoride (PVDF) membrane (Bio-Rad). The membrane was probed with specific monoclonal/polyclonal IgG antibodies directed against the amino acid sequences of unphosphorylated and phosphorylated proteins as follows: mouse anti-NT-4 monoclonal antibody (at a 1:750 dilution; Santa Cruz Biotechnology), goat anti-TrkB polyclonal antibody (at 1:500 dilution; Santa Cruz Biotechnology), rabbit anti-p44/42 MAPK (Erk1/2) monoclonal antibody (at 1:1000 dilution; Cell Signaling, Danvers, MA), rabbit anti-Akt monoclonal antibody (at 1:1000 dilution; Cell Signaling), rabbit anti-phospho-TrkA(Tyr496)/TrkB(tyr516) polyclonal antibody (at 1:1000 dilution; Cell Signaling), rabbit anti-phospho-p44/p42 MAPK(RK1/2) (Thr202/Tyr204) monoclonal antibody (at 1:2000 dilution; Cell Signaling), and rabbit anti-phospho-Akt (Ser473) monoclonal antibody (at 1:2000 dilution; Cell Signaling). Immunoreactive bands were detected using horse-

radish peroxidase (HRP)-conjugated goat anti-mouse, goat anti-rabbit, and donkey anti-goat secondary antibodies (Santa Cruz Biotechnology). Chemiluminescence detection was performed using the ECL Select Detection Kit (GE Healthcare Bio-Sciences AB, Uppsala, Sweden), and bands were subsequently visualized ~~using a~~ using a Gel DOC-It Imaging system (Ultra-Violet Products, Upland, CA). Equal loading in the lanes was evaluated by stripping the blots for 2 hours at 37°C and then overnight at room temperature (IgG Elution Buffer; Thermo Scientific). Reprobing was then performed in an analogous manner with a mouse anti-β2-microglobulin (BMG) monoclonal antibody (Santa Cruz Biotechnology) at a 1:1200 dilution, followed by an HRP-conjugated secondary antibody as described above). Protein levels were analyzed densitometrically in free ImageJ software (version 1.47; http://rsb.info.nih.gov/ij/index.html) and expressed as the relative density in the right eye (experimentally treated retina) versus the left eye (control retina).

Real-Time Quantitative RT-PCR

To analyze the mRNA levels for NT-4, total mRNA was isolated from retinas at 3 months post sodium iodate administration using the PARIS Kit (Life Technologies). Subsequently, the mRNA was reverse-transcribed using the First Strand cDNA Synthesis Kit (Fermentas International, Inc., Burlington, ON, Canada). The quantitative assessment of mRNA levels was performed using a Bio-Rad CFX96 Real-Time PCR Detection System (Bio-Rad). A 15-μL reaction mixture containing 7.5 μL iQ SYBR Green SuperMix (Bio-Rad), 10 ng of complementary DNA (cDNA) template, and 0.9 μM forward and reverse primers for NT-4 and β2-microglobulin (BMG) was prepared, and the cDNA was amplified under the following conditions: 1 cycle at 50°C for 2 minutes and 95°C for 10 minutes, followed by 40 cycles at 95°C for 15 seconds and 60°C for 1 minute. Relative quantification of mRNA expression was calculated using the comparative Ct method. The relative quantitation value of the target, normalized to an endogenous control gene (*BMG*) and relative to a calibrator, was expressed as $2^{-\Delta\Delta Ct}$, where $\Delta Ct = Ct$ of the target genes $- Ct$ of the endogenous control gene, and $\Delta\Delta Ct = \Delta Ct$ of the sample $- \Delta Ct$ of the calibrator.

RNA Isolation, Affymetrix GeneChip Microarray, and Data Analysis

Total RNA was isolated from mouse retinas using the PARIS Kit (Life Technologies) at 3 months post sodium iodate administration. RNA isolates from four retinas were pooled to generate four samples for subsequent experimental procedures. A sense-strand cDNA generated from the total RNA using an Ambion WT Expression Kit (Life Technologies) was subjected to fragmentation and labeling using the GeneChip WT Terminal Labeling Kit (Affymetrix, Santa Clara, CA) and then hybridized onto an Affymetrix WT Array Strip (Affymetrix). Hybridization and subsequent fluidics and scanning steps were performed with an Affymetrix GeneAtlas system (Affymetrix). The differences in expression of the chosen genes and gene ontology (GO) terms were analyzed using the free R statistical programming environment (http://www.r-project.org/) and free Bioconductor packages (http://www.Bioconductor.org).

The differentially expressed genes were classified into functional groups according to the GO analysis.

Electroretinography

Scotopic and photopic ERGs were recorded 3 months after sodium iodate administration. Following overnight dark adaptation, mice were anesthetized with an intraperitoneal injection of ketamine (40 mg/kg) and xylazine (4 mg/kg). Then, the cornea was anesthetized (Alcaine; Alcon Laboratories, Fort Worth, TX), and the pupils were dilated with 1% atropine. Retinal responses were recorded with gold ring contact electrodes (LKC Technologies, Gaithersburg, MD). Needle electrodes placed under the scalp between the eyes and in the tail served as the reference and ground leads, respectively. ERGs were differentially amplified (0.05–1500 Hz), averaged, and stored using an LKC UTAS BigShot System (LKC Technologies). ERGs were recorded in response to strobe flash stimuli presented in the LKC Ganzfeld bowl in a protocol similar to that used for human testing. For the assessment of rod photoreceptor function, a strobe white-flash stimulus was presented to the dark-adapted dilated eye with a low flash intensity (24-dB attenuation), and eight responses recorded at intervals of 8 seconds were computer averaged. Mixed rod and cone responses were obtained using stimulation with white flashes of maximum intensity equal to approximately 1.6 cd*s/m^2 (standard flash [SF], 0-dB attenuation). The retinal responses were measured twice with a 28-second interstimulus interval and averaged. To evaluate the function of cone photoreceptors, animals were light-adapted for 10 minutes under a white background (32 cd/m^2). Next, a strobe white-flash stimulus was presented to the dilated eye in the Ganzfeld bowl using the maximum flash intensity (0-dB attenuation), and responses to eight flashes with an interstimulus interval of 1 second were recorded and averaged. The amplitude of the b-wave was measured from the a-wave trough to the peak of the b-wave or, if an a-wave was not present, from the prestimulus baseline to the peak of the b-wave.

Spectral-Domain Optical Coherence Tomography (SD-OCT) Imaging

To perform the imaging procedures, the pupils of the mice were dilated with 1% atropine. Artificial tears were used throughout the procedure to maintain corneal clarity. Mice were anesthetized with an intraperitoneal injection of ketamine (40 mg/kg) and xylazine (4 mg/kg). Ultrahigh-resolution SD-OCT images were obtained using the Envisu R2200-HR SD-OCT device (Bioptigen, Durham, NC) with the reference arm placed at approximately 1185 mm. SD-OCT images of a specific region of each eye were taken using the optic nerve head as a landmark. Rectangular scans (1.4-mm width, 1000 a-scans/b-scan × 100 frames/b-scan) were obtained while centered on the optic nerve and again with the nerve displaced either temporally/nasally or superiorly/inferiorly.

Statistical Methods

The significance of differences between experimental groups was assessed with the Kruskal-Wallis test followed by the Mann-Whitney test; $P < 0.05$ was considered statistically significant. Data are presented as the mean ± SD. Fisher's exact test was applied for overrepresentation of selected genes in GO biological categories.

Results

Evaluation of Ex Vivo Genetic Modification of MSCs for Therapeutic NT-4 Production

Lentiviral vectors were used to engineer cultured MSCs for the effective production of NT-4 or GFP. First, MSC culture

Investigative Ophthalmology & Visual Science

conditions had to be optimized to achieve a high yield of primary MSCs. From one 75-cm^2 plastic culture flask with confluent adherent cells, approximately 7×10^5 CD45$^-$ MSCs could be obtained in a short period of time. The isolated CD45$^-$ fraction of cultured bone marrow–derived cells presented an MSC phenotype (i.e., plastic adherence and spindle-like shape [Fig. 1C]) and stained positive for Sca-1, CD90, and CD105 with no CD31 expression (Fig. 1D). Next, to transduce the cultured murine MSCs, two recombinant lentiviral vectors expressing human NT-4 (Lv-UbC-NT-4) or GFP (Lv-UbC-GFP) were used (Fig. 1A). Examination at 72 hours after viral transduction showed that GFP-expressing MSCs displayed morphology identical to control cells when examined under phase contrast (Fig. 1E). Following infection with the GFP-encoding lentivirus, GFP-positive MSCs constituted more than 95% of the analyzed MSC population (Fig. 1F). Finally, ELISA results revealed a significant increase in the NT-4 concentration in medium collected from the NT-4–positive MSC culture compared with the uninfected MSC culture or MSCs infected with Lv-UbC-GFP (Fig. 1G).

Homing, Migration, and Survival of Transplanted MSCs Within Injured Retina

We initially sought to determine if MSCs could be efficiently delivered to the retina through intravitreal pars plana injection, and once there, if they could be successfully incorporated into injured retinal tissue. In particular, our goal was to assess the kinetics of MSC trafficking from the vitreous chamber and of integration with the damaged retina. For this reason, we monitored the injected eyes repeatedly in each mouse using SD-OCT. On the seventh day post MSC transplantation, depth-selective SD-OCT fundus images of the vitreous gel revealed hyper-reflective opacities in the vitreous that likely represent injected cells. The opacities were uniformly distributed in the vitreous body and had a homogenous appearance (Fig. 2A). By day 28, the hyper-reflective regions in the vitreous gel disappeared (Fig. 2B). On the third month post injury, en face projection focused on the vitreous body showed that the injected MSCs were absent in the vitreous cavity, and an exact morphology of the vitreous gel was observed that may indicate the effective migration of transplanted MSCs toward the retinal injury (Fig. 2C).

We then evaluated histologic sections to determine the localization of transplanted MSCs in the damaged retina. Experiments using intravitreal transplantation of syngeneic MSCs-GFP into the vitreous cavity of experimental mice allowed us to track the grafted cells. Hence, we used the GFP marker to assess the migration, location, and long-term survival of MSCs after cell grafting. We found that the transplanted cells preferentially migrated toward sites of injured retinal tissue, especially to the RPE and photoreceptor layers, where they were able to survive for up to 3 months (Fig. 2D). A quantitative analysis of the total number of incorporated MSCs-GFP per eye section is summarized in Figure 2E. Of interest, the transplanted MSCs-GFP$^+$ were incorporated in a time-dependent manner, and the greatest number of cells was detected on postinjury day 7, with a subsequent gradual decrease up to the third month post injury. A widespread migration was observed on the seventh day, with a characteristic alignment of spindle-shaped cells in a lateral fashion along the inner nuclear layer of the retina (Fig. 2F). In contrast, at the third month post injury, the vast majority of the injected cells were found to be aligned along the RPE-photoreceptor junction (Fig. 2D). Additionally, to assess the proliferative potential of the transplanted MSCs-GFP, we performed immunohistochemistry against proliferating cell nuclear antigen (PCNA) and found several proliferating cells among the migrating MSCs-GFP in the inner nuclear layer on the seventh day post injection (Fig. 2F). However, we did not detect PCNA$^+$ MSC-GFP cells in third month post transplantation. These results indicate that genetically modified MSCs transplanted into acutely injured retinas may migrate throughout the retinal structures, become integrated within the injured retinal tissue and survive in the posterior segment of the treated eyes for at least 3 months.

Long-Lasting NT-4 Secretion by Engineered MSCs and Local Induction of Prosurvival Signaling in Injured Retinas

At 3 months post transplantation, the expression of NT-4 was analyzed in retinas collected from the right eyes, treated with transduced MSC-NT-4 and compared with retinas from the corresponding left eyes, which had been injected with uninfected MSCs and served as controls. After the injection of uninfected MSCs into the vitreous cavity, the NT-4 levels in the retina were very low, both at the mRNA (Fig. 3A) and protein (Fig. 3B) levels. In contrast, the retinas of the right eyes injected with NT-4–transduced MSCs revealed a significant increase in NT-4 protein, as detected in Western blot analysis (Fig. 3B). Similarly, the NT-4 mRNA level was increased in the eyes treated with MSC-NT-4 compared with those injected with uninfected MSCs (Fig. 3A).

Next, we sought to examine whether locally released NT-4 possesses biological activity and is able to induce a specific response in the target cells. Hence, we analyzed the expression of an active form of the TrkB receptor by determining the Trk tyrosine phosphorylation in immunoblots of lysates from retinas treated with MSC-NT-4 and compared this expression level with that in retinas injected with uninfected MSCs. We found that MSC-NT-4 transplantation elicited a strong increase in TrkB phosphorylation in injured retinas without affecting the total TrkB level (Fig. 3C). This finding indicates that NT-4 binds excessively to its specific receptor and activates it. Additionally, to determine the precise localization of the target cells, we performed an immunofluorescence analysis of retinas collected from MSC-NT-4–treated mice using an anti-TrkB antibody. We found that TrkB expression in the retina after MSC-NT4 transplantation was limited to the RPE/photoreceptor junction (Fig. 3D). These results show the potential target cells for NT-4 activity locally released from MSC-NT-4 at the site of injury.

Furthermore, to determine whether the TrkB-dependent signal transduction pathway is biologically active 3 months after MSC-NT-4 transplantation, we probed the immunoblots of lysates from retinas treated with MSC-NT-4 with antibodies against the phosphorylated and total forms of selected members of this signaling pathway, such as pAkt^{Ser473} and Akt, as well as representatives of the MAPK family—pERK-1^{Thr202}/pERK-1^{Tyr204} and ERK1/2. Indeed, a densitometric analysis demonstrated significant increases in the expression levels of phosphorylated Akt and ERK1/2 in the retinas of MSC-NT-4–treated mice compared with those in control retinas (Figs. 3E, 3F). These data suggest that the NT-4 released from engineered MSCs is highly bioactive and may induce the continuous activation of Akt and MAPK-related pathways during long-term observation and thus contribute to the neuroprotective and survival functions of TrkB-related signaling. Altogether, the above results confirm the long-lasting in vivo biological effect of ex vivo-engineered MSCs using lentiviral vectors specifically constructed to express the therapeutic *NT-4* gene.

Investigative Ophthalmology & Visual Science

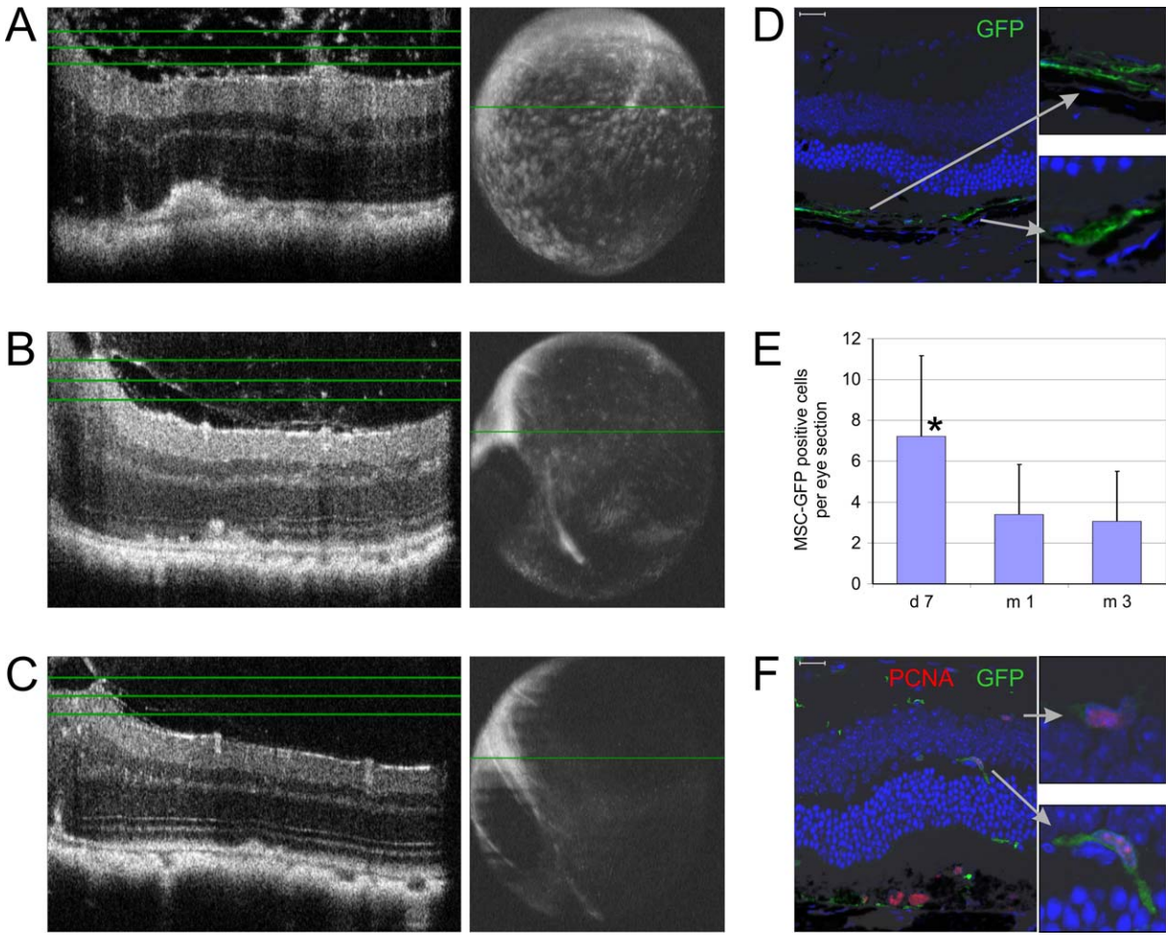

Figure 2. Longitudinal follow-up of MSC fate at different time points post intravitreal transplantation. A representative SD-OCT image of an injured retina on the seventh day post MSC-NT-4 transplantation (**A**). The *green lines* on the OCT images (at the left side) indicate the boundaries of tissue depth displayed in an en face two-dimensional fundus projection (at the right side). The depth-dependent fundus image at this time point shows injected cells in the vitreous. The cells were uniformly distributed and had a homogenous appearance. The SD-OCT analyses on the 28th day (**B**) and third month (**C**) show the absence of injected MSCs in the vitreous cavity. Immunofluorescence analysis of retinas after intravitreal MSC-GFP delivery showing transplanted cells (*green*) that survived in the posterior eyecup up to 3 months post transplantation (**D**). Quantitative analysis of the total number of incorporated MSCs per eye section ($n = 5$) (**E**). Double-stained sections (for GFP and PCNA) were used to visualize and localize proliferating MSCs (**F**). *Scale bar*: 20 μm. $^*P < 0.05$ for day 7 versus other time points ($n = 5$/time point).

Improvement of Retinal Function and Morphology After MSC-NT-4 Treatment During Long-Term Observation

To assess whether the local production of NT-4 was associated with positive and prolonged changes in retinal function, we evaluated the bioelectrical retinal response at 3 months after sodium iodate administration and MSC-NT-4 transplantation. The changes in the scotopic and photopic ERGs between MSC-NT-4–treated right eyes and left eyes injected with uninfected MSCs are summarized in Figure 4. ERG analysis revealed significant preservation of retinal bioelectrical activity in eyes that received MSC-NT-4 injection compared with eyes that received uninfected control MSCs. In the analysis of the scotopic response 3 months after transplantation, in MSC-NT-4–recipient right eyes, the ERG response appeared to be substantially restored, as b-wave amplitude rose significantly ($P < 0.05$) compared with the corresponding left eyes (Fig. 4A). This result may indicate a significant improvement in the rod cell–mediated response. Similar recovery trends were observed in the analysis of oscillatory potentials (Fig. 4B). Of interest, when analyzing dark-adapted eyes stimulated with white flashes of maximum intensity, no statistically significant difference was observed between eyes treated with MSC-NT-4 and uninfected MSCs, despite a trend toward higher b-wave amplitudes in the NT-4–treated group (Fig. 4C). Similarly, when analyzing the cone cell–mediated response, we observed no difference in the b-wave amplitude between MSC-NT-4–treated and control eyes (Fig. 4D). An immunofluorescence analysis showed that $NaIO_3$-mediated retinal injury reduced the overall length of the rod outer segments (OS) and resulted in substantial red/green cone disorganization. Subsequently, NT-4–mediated rescue involved mostly rod photoreceptors but did not significantly influence the red/green-cone photoreceptor cell population (Figs. 4E, 4F). This may indicate that cones are more susceptible to disruption than rods, possibly owing to structural or physiological differences in these two cell types, and the administered therapy had a greater impact on rod- than on cone-photoreceptor cell defects.

To determine if the therapeutic intervention had an impact on the retinal structure, we used OCT to assess the retinal morphology at the third month post $NaIO_3$ administration and MSC transplantation (Fig. 4G). The OCT images obtained from MSC-NT-4–treated right eyes showed a complete restoration of

Investigative Ophthalmology & Visual Science

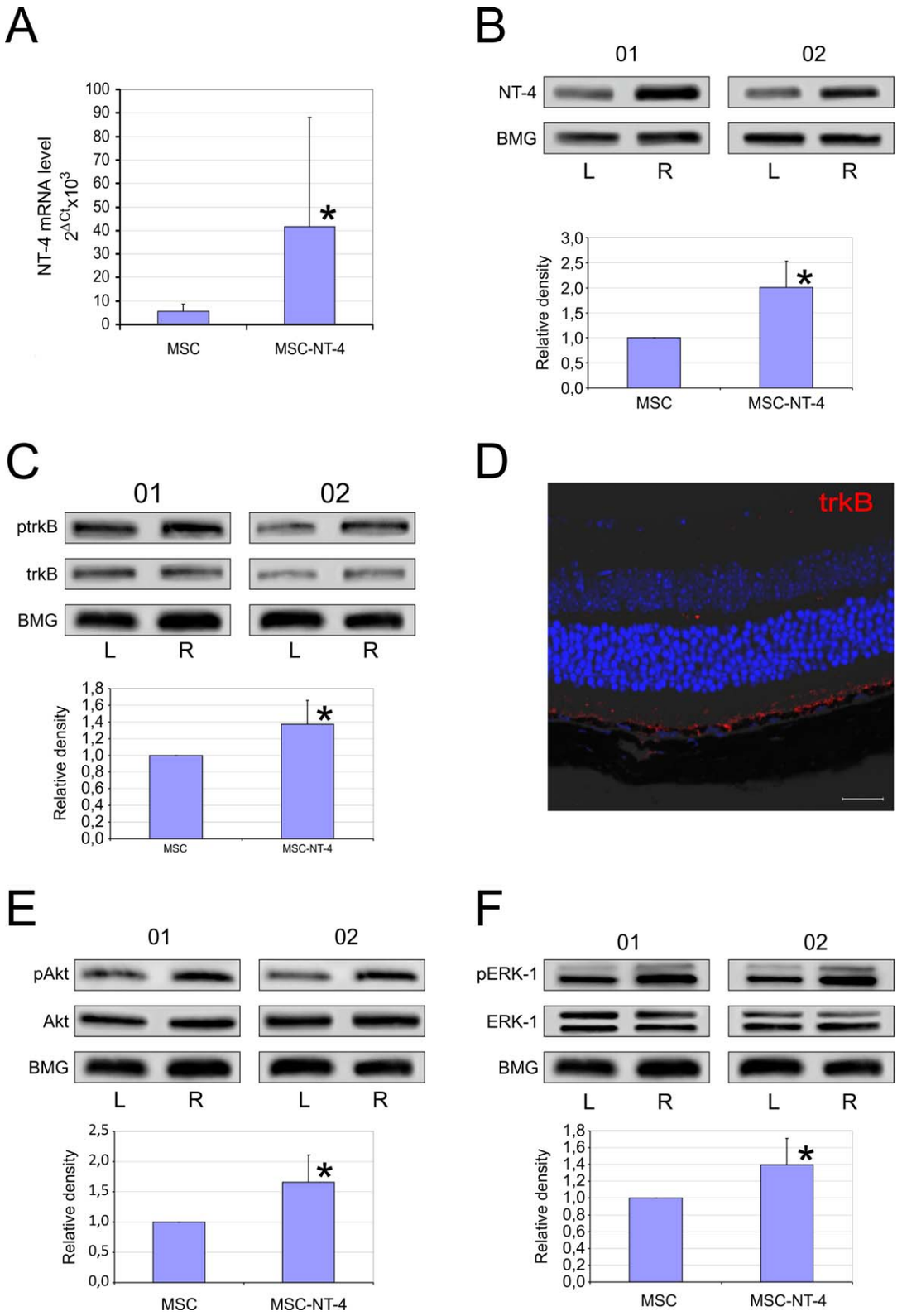

Figure 3. Long-lasting NT-4 expression and its biological activity in retinal cells. NT-4 mRNA (**A**) and NT-4 protein (**B**) expression were detected in the right eyes treated with MSCs-NT-4, and their levels were significantly increased compared with those in the control left eyes at the third month post transplantation. Representative Western blot analysis and densitometry for relative protein quantification of the phosphorylated forms of $TrkA^{Tyr496}$/$TrkB^{Tyr516}$ (**C**), Akt^{Ser473} (**E**), and ERK-1^{Thr202}/ERK-1^{Tyr204} (**F**) following MSC-NT-4 transplantation. The 90, 60, and 42/44 kDa bands are considered to be phospho-TrkB, Akt, and ERK-1, respectively. The 12 kDa band is BMG, which was used as an internal control. Immunoblotting demonstrated strong expression of the active, phosphorylated forms of TrkB, Akt, and ERK-1 in the retinas collected from MSC-NT-4–treated mice.

Investigative Ophthalmology & Visual Science

Mean values ± SDs of triplicate measurements for each phosphorylated protein normalized to BMG are presented in the diagrams under the blot photographs ($n = 5$). L, left eye; R, right eye; 01, 02 indicate unique mouse numbers. The results are representative of three independent experiments. Immunofluorescent localization of TrkB protein in retinas treated with MSC-NT-4 showed that its expression is limited to the RPE/photoreceptor junction, especially at the sites of injury (**D**). *Scale bar*: 20 μm.

the laminated organization of the outer retina. At the site of injury, we discerned hyper-reflective flecks at the RPE-photoreceptor junction as well as an irregular RPE band with areas of local thickening and thinning. However, the hyper-reflective bands in the outer retina ascribed to the external limiting membrane (ELM), inner segments (IS), and OS were visible, indicating that photoreceptor cells regained their morphology. In contrast, in the control left eyes, which were injected with uninfected MSCs at this time point, we detected the disintegration of the outer retinal zone architecture. In addition, the ELM was not visible, and the pair of bright bands corresponding to both the IS and OS were disorganized.

Candidate Genes and Pathways for Retinal Neuroregeneration Induced by Long-Term Therapy With NT-4

Next, we continued to characterize the neuroprotective effect of long-lasting NT-4 secretion by analyzing the global gene expression profiles of retinas collected at 3 months post injury. Microarray comparisons of retinas from MSC-NT-4–treated right eyes versus control uninfected MSC-treated left eyes at this time point revealed that 31 genes were at least 2-fold upregulated. In contrast, the same analysis revealed that only five genes were at least 2-fold downregulated in the eyes treated with engineered MSCs. The top 10 upregulated genes and the 5 downregulated genes with at least a 2-fold change in their expression at 3 months post injury are presented in Supplementary Tables S1 and S2, respectively. The most upregulated genes included Serpine3 (*Serpine3*; 9.9-fold) and Serpine1 (*Serpine1*; 4.16-fold), which are both members of the serine (or cysteine) proteinase inhibitor family and the MAPK signaling pathway, and endothelin-2 (*Edn2*; 2.96-fold), a member of the endothelin protein family of secretory vasoconstrictive peptides that is also involved in the stimulation of cell growth and division. Of importance, the analysis identified significant increases (at least a 2-fold change) in the expression of the crystallin gene superfamily, represented by the β and γ members including *Cryba4*, *Crybb3*, *Cryba2*, *Crybb1*, *Crybb2*, *Cryba1*, and *Crygc*. Thus, it appears that a select group of crystallins is differentially affected by NT-4 cell– and gene-based therapy. Of interest, one of the top upregulated genes (a 2.6-fold increase) at 3 months post injury was glial fibrillary acidic protein (GFAP), which is a cytoskeletal protein normally expressed at low levels by astrocytes and the end-feet of Müller cells but which is a marker of glial-cell activation when overexpressed. The three most downregulated genes included Ras-related protein Rab-14 (*Rab14*; −3.45-fold), a member of the RAS oncogene family involved in intracellular membrane trafficking; heterochromatin protein 1 binding protein 3 (*Hp1bp3*; −2.73-fold), which is involved in chromatin structure and function; and anaphase-promoting complex subunit 1 (*Anapc1*; −2.18), a member of the E3 ubiquitin ligase complex that regulates progression through metaphase to the anaphase portion of the cell cycle.

To more closely examine the NT-4–dependent signaling network, we analyzed the expression of a number of members of signal transduction pathways related to the TrkB receptor and its ligand, NT-4. Among the upregulated gene transcripts, we observed several genes and complexes of genes, such as *Irs*, *Sos*, and *Ras*, that are normally related to intracellular kinase cascades, such as MAPK and Akt, and are known to robustly affect cell survival, growth, or differentiation. In this context, our results suggest that NT-4 is important for the regulation of signaling pathways required for cell proliferation and the restoration of cell functions such as axonogenesis after injury. Furthermore, the specific cellular delivery of NT-4 had a positive impact on the expression of anti-apoptotic Bcl-2 and Birc proteins. The proposed NT-4–mediated signaling pathway analysis is schematically presented in Figure 5. The color coding shows the dynamics of the gene expression changes, whereby red represents upregulation and green represents downregulation.

Next, all the differentially expressed genes were classified according to their GO classification of biological processes. Functional analysis using these GO terms revealed that a number of specific pathways were strongly involved in the observed NT-4–mediated regeneration process after acute retinal $NaIO_3$-induced damage. As summarized in Supplementary Table S3, the following five biological processes were significantly upregulated: eye development (7 genes of 255); sensory organ development (8 genes of 415); visual perception (7 genes of 121); sensory perception of light stimulus (7 genes of 121); and system development (13 genes of 2759).

Discussion

Retinal degeneration is caused by a series of metabolic and histologic changes in the retina and underlying tissues, which culminate in progressive retinal atrophy and, in the most severe form, total degeneration of functional photoreceptors, producing gradual vision deterioration and subsequent blindness. Current medical and surgical interventions for retinal degeneration are focused on the modification of intrinsic and extrinsic etiologic factors that could prevent the progression of vision loss, such as the delivery of vital growth factors, increasing blood flow into retinal tissue, or pharmacologic inhibition of cellular senescence and the resulting oxidative damage. With these issues in mind, in the present study, we transplanted ex vivo modified MSC-NT-4 to protect injured retinal tissue in mice. We found that MSCs survived for at least 3 months after intravitreal injection and preferentially migrated toward sites of injury, leading to the morphologic and functional recovery of damaged retinal cells. Moreover, we observed that the specific cellular delivery of NT-4 had a positive impact on the activation of signal transduction pathways that are important for neural cell survival, growth, and differentiation.

Various growth factors have been tested in animal models of nervous-tissue degeneration and retinal damage as possible therapeutic agents for preserving the function and structure of injured tissues, with a particular focus on the use of NTs.[42–44] The NT family is essential for neuronal survival, development, and functional maintenance of the CNS, and its members include NGF, BDNF, NT-3, and NT-4. Two NTs, BDNF and NT-4, bind to the TrkB receptor,[7] and these are extensively distributed in the developing and mature nervous system, being most critical for neuron development, survival, and neural tissue repair.[47] Neurotrophin-4 and other NTs play an important role in neuronal survival, and their downregulation is thought to lead to neural degeneration.[48] Furthermore, NT-4 knockout mice have been shown to recapitulate the degener-

Investigative Ophthalmology & Visual Science

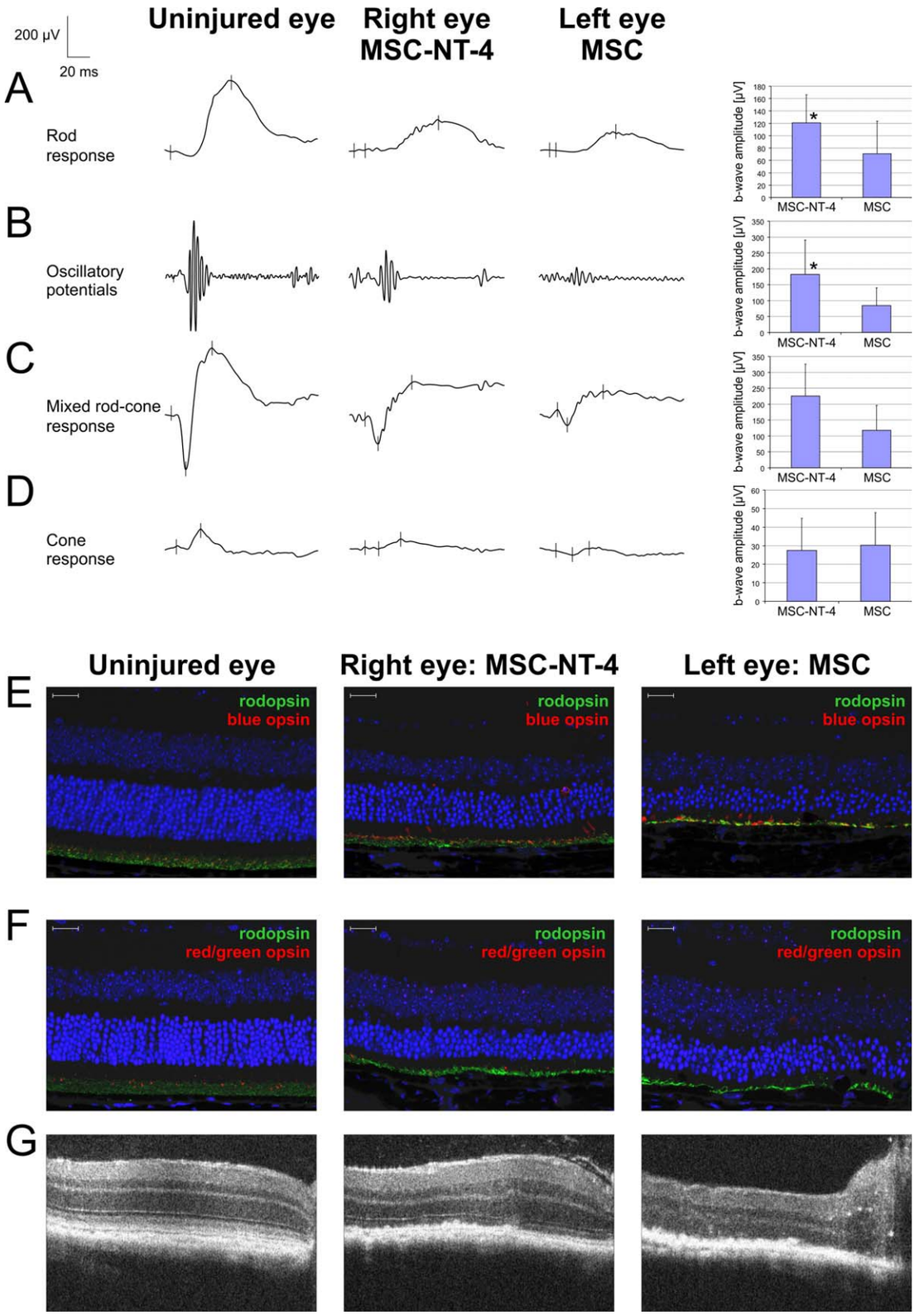

Figure 4. Effects of in vivo experimental therapy with MSC-NT-4 on retinal morphology and ERG amplitudes at 3 months post injury. The rod (**A**), mixed rod-cone (**C**), and cone (**D**) responses were analyzed in addition to the oscillatory potentials (OP) and high-frequency and low-amplitude potentials superimposed on the rising phase of the b-wave (**B**). The representative ERG responses recorded at 3 months post MSC-NT-4 therapy are shown. The b-wave amplitude measurements are presented as the mean ± SD. Analysis of co-immunoreactivity of rhodopsin with blue-opsin (**E**) or rhodopsin with red/green-opsin (**F**) by immunofluorescence labeling. Representative in vivo SD-OCT images of the retina at the third month post injury (**G**) showing a considerable improvement in the architecture of the outer and inner photoreceptor segments of the right eyes treated with MSC-NT-4. *Scale bar*: 20 µm. *$P < 0.05$ for MSC-NT-4 injection into the right eye versus transplantation of uninfected MSCs into the left eye at 3 months post cell transplantation ($n = 5$).

Investigative Ophthalmology & Visual Science

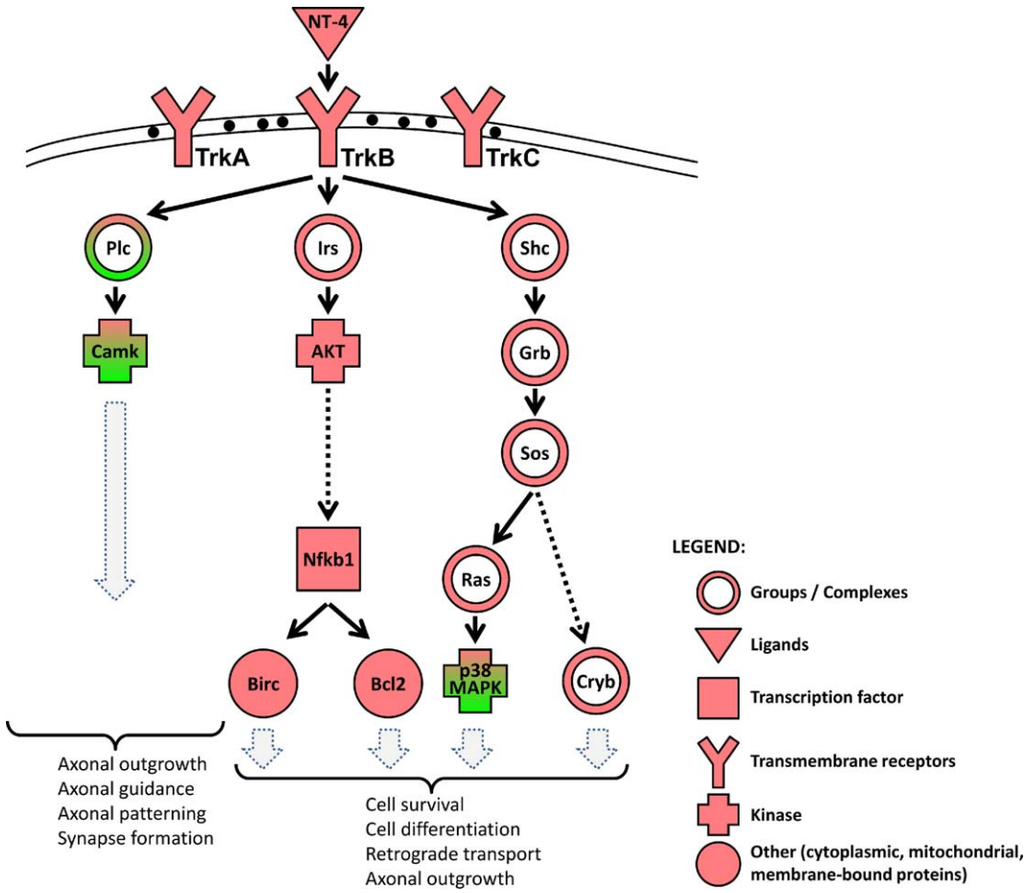

Figure 5. NT-4–mediated signaling pathway analysis at 3 months post MSC-NT-4 therapy in an acute retinal injury model. *Red*: upregulated genes; *green*: downregulated genes.

ation observed in NT deficiencies,[49] which suggests that decreased levels of NT-4 may play an important role in neuropathology. As all NTs have a short half-life in vivo and may not easily permeate the blood-brain barrier, their administration either intravenously or locally is unlikely to produce long-term therapeutic results. In contrast, the transduction of NT genes into stem cells such as MSCs may ensure sufficient and steady NT expression by those cells. In the current study, we generated genetically modified MSCs to deliver NT-4 and showed that this approach has the potential to improve bioelectrical function in a mouse model of acute retinal injury.

Lentiviruses are one of the most frequently employed viral vectors in stem cell–based therapy because they are capable of transferring exogenous genes into the genomes of MSCs to induce their stable expression.[32] To assess the infectivity and the potential nonspecific effects of the constructed lentiviral vectors on transduced MSCs, we used Lv-UbC-GFP encoding the reporter GFP transgene to infect murine MSCs. In our study, the average infection rate reached approximately 95% of the total number of cultured MSCs. Moreover, the transduced MSCs presented viability and morphology characteristics similar to those of uninfected cells. These results demonstrate that the lentiviral vectors used in this study for the infection of cultured murine MSCs offer a highly sophisticated tool for ex vivo MSC engineering for subsequent cell- and gene-based therapy. Likewise, for the therapeutic protocol, we infected cultured murine MSCs with the *NT-4* gene using Lv-UbC-NT-4 and confirmed the significant increase in the in vitro production of NT-4 protein by these cells compared with uninfected MSCs. The amount of NT-4 secreted was high and was a reflection of successful MSC transduction. Under these circumstances, the in vivo results obtained at 3 months post transplantation revealed that NT-4 delivered from engineered MSC-NT-4 provided a long-lasting contribution to the intrinsic mechanisms governing repair of the local nervous system after retinal chemical injury. Of importance, we found that intravitreally transplanted MSCs successfully integrated within the injured retinal tissue. These results are consistent with previous studies demonstrating that lentivirally transduced MSCs are able to survive and to express transgenes following transplantation.[50] Of interest, in the present case, we observed an improvement in retinal function via ERG, which indirectly indicates that the administration of MSC-NT-4 may promote retinal cell survival and substantially decrease the severity of photoreceptor and RPE damage in this animal model of acute retinal injury.

Based on the findings described above, we hypothesize that ocular expression of NT-4, mediated by the local transplantation of genetically engineered MSCs, may provide a basis for the prolonged preservation of gradually degenerating retinal cells. The benefits observed in the MSC-NT-4 group appear to be related to increased retinal cell survival, and this hypothesis is consistent with our recent results demonstrating histologic RPE regeneration and substantial improvement of the ERG response at 3 months after retinal injury induced by low-dose $NaIO_3$ administration (15 mg/kg of body weight).[51] In this previous study, we provided novel compelling evidence of the

Investigative Ophthalmology & Visual Science

crucial role of NTs in retinal repair and identified the signaling pathways that are activated during this process. The genes that appeared to be essential for the survival and regeneration of injured photoreceptors and other retinal neurons, those responsible for nervous-tissue remodeling and neuron development, the regulation of synaptic transmission, and the establishment of localization, were substantially induced by the third month after injury. Thus, our previous results indicate that the overexpression of NTs in glial cells may instigate multifaceted genomic changes responsible for the observed improvement in visual function.[51]

The results of our present study show that transplantation of MSCs highly expressing *NT-4* leads to prolonged local expression of NT-4 protein in retinal tissue and a marked improvement in the long-term ERG response. Although the underlying mechanisms for these beneficial effects have not been well described, the present findings support the notion that the ameliorative effects of MSC-NT-4 transplants are a result of their ability to modulate the expression of several genes and, subsequently, signal transduction pathways important for neural cell survival, growth, and differentiation. Likewise, we were able to detect considerably increased expression of several mRNA encoding proteins, such as Irs, Sos, and Ras, belonging to MAPK- or AKT-related pathways that are known to contribute to neural cell survival. Furthermore, the specific cellular delivery of NT-4 had a positive impact on the expression of the anti-apoptotic proteins Bcl-2 and Birc.

Of interest, using comprehensive RNA microarray analyses, we also showed that the improvement in retinal function after MSCs-NT-4 therapy was accompanied by coordinated mRNA upregulation of several members of both the β- and γ-crystallin superfamilies. Our analysis of the global gene expression changes suggested that the observed gene expression alterations could be categorized into two genetic patterns: one related to neuron growth and elongation through axonogenesis, including the β- and γ-crystallin genes (*Cryba4*, *Crybb3*, *Cryba2*, *Crybb1*, *Crybb2*, *Cryba1*, and *Crygc*) and the *Serpine3* gene; and another related to the activation of retinal glial cells and the regulation of cell proliferation, including the *GFAP*, *Serpine1*, *Serpine3*, and *Edn2* genes.

Although crystallins derive their name from their initial discovery in the lens, they serve many extralenticular functions.[52,53] Recently, several studies have indicated that crystallins play an important protective and therapeutic role in neurodegenerative diseases such as Parkinson's disease, Alzheimer's disease, and multiple sclerosis.[54] Similarly, the high abundance of numerous crystallins within the retina also points to their vital functions in protecting retinal cells from various insults, and there is a large body of evidence supporting their protective activities in human eye diseases such as ischemic-reperfusion, AMD, retinopathy of prematurity, optic nerve injury, mechanical trauma, light injury, uveitis, endophthalmitis, and diabetic retinopathy.[55] Furthermore, microarray analysis revealed that mouse retinal cells express transcripts for several members of the crystalline gene family.[56] The gene products for αA-, αB-, β-, and γ-crystallins were localized in the inner and outer nuclear layers, suggesting that crystallins play vital functions in protecting retinal cells from damage from environmental and/or metabolic stress.[55] Of interest, Crybb2 has been specifically implicated in the regrowth of retinal ganglion cell axons, which suggests that β-crystallins may constitute a new group of factors that operate either directly or indirectly on neurons to promote axon outgrowth.[57] In addition, it has been shown that intravitreal injections of β-crystallin strongly enhanced axon regeneration when retinal explants were grown in culture.[58] The pancytoprotective properties of β-crystallins were confirmed recently by Böhm et al.,[59] who found that both β-crystallins, CrybB2 and CrybB3, strongly protected RPE from induced stress in vitro and in vivo. Moreover, the same group found that most ocular cells responded to the appearance of CrybB2, resulting in marked changes in the expression of certain proteins, including rhodopsin (photoreceptors), vimentin (retinal glial cells), and Iba-1 (microglia). Of importance, photoreceptors displayed an improved survival rate following CrybB2 administration in vivo in comparison to the control group.[60]

Much less is known about the potential activity network between different crystallins and neurotrophic factors in the retina. The presence of such a network between several NTs and β-crystallins in retinal cells was recently confirmed in both in vitro and in vivo studies. Böhm et al.[59] found that the level of glial-derived ciliary neurotrophic factor (GDNF) expression by cultured human ARPE-19 cells was strongly dependent on external *Crybb3* application to the extracellular microenvironment. Similarly, Fischer et al.[58] showed that ciliary neurotrophic factor (CNTF) was produced in retinal organotypic explants in response to substitution with crystallins. Furthermore, this group also confirmed that crystallins β and γ further promote the growth of retinal neurons by enhancing the local production of CNTF in vivo and in vitro.[61] In contrast, the highly coordinated local expression of β- and γ-crystallins in eyes exposed to NT-4–combined cell- and gene-based therapy suggests the existence of NT-regulated mechanisms of crystallin production and their subsequent role in retinal neuron cell regeneration. We hypothesize that exogenous NT-4 activates a signaling cascade that enhances retinal regeneration after injury and that crystallins play a key role in this process. As demonstrated in our study, the emerging model highlights β- and γ-crystallins as key factors supporting retinal repair. Furthermore, the results of our microarray comparisons raised the possibility that neuronal crystallins may constitute a novel class of neuron growth-promoting factors, and this possibility could lead to novel therapeutic opportunities for a wide range of retinal disorders.

Together, our results suggest that NT-4 cell- and gene-combined therapy may constitute a new therapeutic strategy operating either directly or indirectly on retinal neurons and RPE cells to promote their survival and neuroprotection during the course of acute chemical damage to the murine retina. However, irrespective of the mechanism operating at the level of injured retinal cells, the factors mediating either NT-related therapeutic effects or the upregulation of β- and γ-crystallin expression in retinal tissue remain to be elucidated. We propose that genetically engineered MSCs may be considered a cell-based therapy for retinal degenerative diseases such as AMD or retinitis pigmentosa when the risk-benefit ratio has been carefully considered. Our in vivo system based on lentiviral vector-modified MSCs has been shown to be a valuable approach that may be considered for future human gene therapy applications in clinical ophthalmology.

Acknowledgments

The authors thank Maciej Wiznerowicz for the kind gift of psPAX2 and pMD2.G plasmids.

Supported by National Science Center Grant No. N N402 665440 (AM) and European Union structural funds—Innovative Economy Operational Program POIG.01.01.02-00-109/09-00 (JD).

Disclosure: **A. Machalińska**, None; **M. Kawa**, None; **E. Pius-Sadowska**, None; **J. Stępniewski**, None; **W. Nowak**, None; **D. Rogińska**, None; **K. Kaczyńska**, None; **B. Baumert**, None; **B. Wiszniewska**, None; **A. Józkowicz**, None; **J. Dulak**, None; **B. Machaliński**, None

Investigative Ophthalmology & Visual Science

References

1. Karl MO, Reh TA. Regenerative medicine for retinal diseases: activating endogenous repair mechanisms. *Trends Mol Med*. 2010;16:193–202.
2. de Oliveira Dias JR, Rodrigues EB, Maia M, Magalhães O Jr, Penha FM, Farah ME. Cytokines in neovascular age-related macular degeneration: fundamentals of targeted combination therapy. *Br J Ophthalmol*. 2011;95:1631–1637.
3. Bull ND, Martin KR. Concise review: toward stem cell-based therapies for retinal neurodegenerative diseases. *Stem Cells*. 2011;29:1170–1175.
4. Skaper SD. The biology of neurotrophins, signalling pathways, and functional peptide mimetics of neurotrophins and their receptors. *CNS Neurol Disord Drug Targets*. 2008;7:46–62.
5. Cui Q. Actions of neurotrophic factors and their signaling pathways in neuronal survival and axonal regeneration. *Mol Neurobiol*. 2006;33:155–179.
6. Zeng W, Wen C, Wu Y, et al. The use of BDNF to enhance the patency rate of small-diameter tissue-engineered blood vessels through stem cell homing mechanisms. *Biomaterials*. 2012; 33:473–484.
7. Dechant G. Molecular interactions between neurotrophin receptors. *Cell Tissue Res*. 2001;305:229–238.
8. Patapoutian A, Reichardt LF. Trk receptors: mediators of neurotrophin action. *Curr Opin Neurol*. 2001;11:272–280.
9. Franke TF, Yang SI, Chan TO, et al. The protein kinase encoded by the Akt proto-oncogene is a target of the PDGF-activated phosphatidylinositol 3-kinase. *Cell*. 1995;81;727–736.
10. Dudek H, Datta SR, Franke TF, et al. Regulation of neuronal survival by the serine-threonine protein kinase Akt. *Science*. 1997;275:661–665.
11. Hetman M, Xia Z. Signaling pathways mediating anti-apoptotic action of neurotrophins. *Acta Neurobiol Exp*. 2000;60:531–545.
12. Raman M, Chen W, Cobb MH. Differential regulation and properties of MAPKs. *Oncogene*. 2007;26:3100–3112.
13. Bennett JL, Zeiler SR, Jones KR. Patterned expression of BDNF and NT-3 in the retina and anterior segment of the developing mammalian eye. *Invest Ophthalmol Vis Sci*. 1999;40:2996–3005.
14. Oku H, Ikeda T, Honma Y, et al. Gene expression of neurotrophins and their high-affinity Trk receptors in cultured human Müller cells. *Ophthalmic Res*. 2002;34:38–42.
15. Lambert WS, Clark AF, Wordinger RJ. Neurotrophin and Trk expression by cells of the human lamina cribrosa following oxygen-glucose deprivation. *BMC Neurosci*. 2004;5:51.
16. Sawai H, Clarke DB, Kittlerova P, Bray GM, Aguayo AJ. Brain-derived neurotrophic factor and neurotrophin-4/5 stimulate growth of axonal branches from regenerating retinal ganglion cells. *J Neurosci*. 1996;16:3887–3894.
17. Vecino E, García-Crespo D, García M, Martinez-Millán L, Sharma SC, Carrascal E. Rat retinal ganglion cells co-express brain derived neurotrophic factor (BDNF) and its receptor TrkB. *Vision Res*. 2002;42:151–157.
18. Spalding KL, Rush RA, Harvey AR. Target-derived and locally derived neurotrophins support retinal ganglion cell survival in the neonatal rat retina. *J Neurobiol*. 2004;60:319–327.
19. Seki M, Tanaka T, Sakai Y, et al. Müller cells as a source of brain-derived neurotrophic factor in the retina: noradrenaline upregulates brain-derived neurotrophic factor levels in cultured rat Müller cells. *Neurochem Res*. 2005;30:1163–1170.
20. Peterson WM, Wang Q, Tzekova R, Wiegand SJ. Ciliary neurotrophic factor and stress stimuli activate the Jak-STAT pathway in retinal neurons and glia. *J Neurosci*. 2000;20: 4081–4090.
21. Harada T, Harada C, Nakayama N, et al. Modification of glial-neuronal cell interactions prevents photoreceptor apoptosis during light-induced retinal degeneration. *Neuron*. 2000;26: 533–541.
22. Walsh N, Valter K, Stone J. Cellular and subcellular patterns of expression of bFGF and CNTF in the normal and light stressed adult rat retina. *Exp Eye Res*. 2001;72:495–501.
23. Turner BA, Sparrow J, Cai B, Monroe J, Mikawa T, Hempstead BL. TrkB/BDNF signaling regulates photoreceptor progenitor cell fate decisions. *Dev Biol*. 2006;299:455–465.
24. Ghazi-Nouri SM, Ellis JS, Moss S, Limb GA, Charteris DG. Expression and localisation of BDNF, NT4 and TrkB in proliferative vitreoretinopathy. *Exp Eye Res*. 2008;86:819–827.
25. Taylor S, Srinivasan B, Wordinger RJ, Roque RS. Glutamate stimulates neurotrophin expression in cultured Müller cells. *Brain Res Mol Brain Res*. 2003;111:189–197.
26. García M, Vecino E. Role of Müller glia in neuroprotection and regeneration in the retina. *Histol Histopathol*. 2003;18:1205–1218.
27. Zigova T, Pencea V, Wiegand SJ, Luskin MB. Intraventricular administration of BDNF increases the number of newly generated neurons in the adult olfactory bulb. *Mol Cell Neurosci*. 1998;11:234–245.
28. Di Polo A, Aigner LJ, Dunn RJ, Bray GM, Aguayo AJ. Prolonged delivery of brain-derived neurotrophic factor by adenovirus-infected Müller cells temporarily rescues injured retinal ganglion cells. *Proc Natl Acad Sci U S A*. 1998;95:3978–3983.
29. Clarke DB, Bray GM, Aguayo AJ. Prolonged administration of NT-4/5 fails to rescue most axotomized retinal ganglion cells in adult rats. *Vision Res*. 1998;38:1517–1524.
30. Peinado-Ramón P, Salvador M, Villegas-Pérez MP, Vidal-Sanz M. Effects of axotomy and intraocular administration of NT-4, NT-3, and BDNF on the survival of adult rat retinal ganglion cells: a quantitative in vivo study. *Invest Ophthalmol Vis Sci*. 1996;37: 489–500.
31. Guerin MB, McKernan DP, O'Brien CJ, Cotter TG. Retinal ganglion cells: dying to survive. *Int J Dev Biol*. 2006;50:665–674.
32. Huang B, Tabata Y, Gao JQ. Mesenchymal stem cells as therapeutic agents and potential targeted gene delivery vehicle for brain diseases. *J Control Release*. 2012;162:464–473.
33. Wang S, Lu B, Girman S, et al. Non-invasive stem cell therapy in a rat model for retinal degeneration and vascular pathology. *PLoS One*. 2010;5:e9200.
34. Zhang, Y, Wang, W. Effects of bone marrow mesenchymal stem cell transplantation on light-damaged retina. *Invest Ophthalmol Vis Sci*. 2010;51:3742–3748.
35. Lu B, Wang S, Girman S, McGill T, Ragaglia V, Lund R. Human adult bone marrow-derived somatic cells rescue vision in a rodent model of retinal degeneration. *Exp Eye Res*. 2010;91: 449–455.
36. Johnson TV, Bull ND, Hunt DP, Marina N, Tomarev SI, Martin KR. Neuroprotective effects of intravitreal mesenchymal stem cell transplantation in experimental glaucoma. *Invest Ophthalmol Vis Sci*. 2010;51:2051–2059.
37. Meyerrose T, Olson S, Pontow S, et al. Mesenchymal stem cells for the sustained in vivo delivery of bioactive factors. *Adv Drug Deliv Rev*. 2010;62:1167–1174.
38. Conget PA, Minguell JJ. Adenoviral-mediated gene transfer into ex vivo expanded human bone marrow mesenchymal progenitor cells. *Exp Hematol*. 2000;28:382–390.
39. Allay JA, Dennis JE, Haynesworth SE, et al. LacZ and interleukin-3 expression in vivo after retroviral transduction of marrow-derived human osteogenic mesenchymal progenitors. *Hum Gene Ther*. 1997;8:1417–1427.

40. Marx JC, Allay JA, Persons DA, et al. High-efficiency transduction and long-term gene expression with a murine stem cell retroviral vector encoding the green fluorescent protein in human marrow stromal cells. *Hum Gene Ther*. 1999;10:1163–1173.
41. McGinley L, McMahon J, Strappe P, et al. Lentiviral vector mediated modification of mesenchymal stem cells & enhanced survival in an in vitro model of ischaemia. *Stem Cell Res Ther*. 2011;2:12.
42. Harper MM, Adamson L, Blits B, Bunge MB, Grozdanic SD, Sakaguchi DS. Brain-derived neurotrophic factor released from engineered mesenchymal stem cells attenuates glutamate- and hydrogen peroxide-mediated death of staurosporine-differentiated RGC-5 cells. *Exp Eye Res*. 2009;89:538–548.
43. Shi D, Chen G, Lv L, et al. The effect of lentivirus-mediated TH and GDNF genetic engineering mesenchymal stem cells on Parkinson's disease rat model. *Neurol Sci*. 2011;32:41–51.
44. Tao J, Ji F, Liu B, Wang F, Dong F, Zhu Y. Improvement of deficits by transplantation of lentiviral vector-modified human amniotic mesenchymal cells after cerebral ischemia in rats. *Brain Res*. 2012;1448:1–10.
45. Lois C, Hong EJ, Pease S, Brown EJ, Baltimore D. Germline transmission and tissue-specific expression of transgenes delivered by lentiviral vectors. *Science*. 2002;295:868–872.
46. Zhu H, Guo ZK, Jiang XX, et al. A protocol for isolation and culture of mesenchymal stem cells from mouse compact bone. *Nat Protoc*. 2010;5:550–560.
47. Murer MG, Yan Q, Raisman-Vozari R. Brain-derived neurotrophic factor in the control human brain, and in Alzheimer's disease and Parkinson's disease. *Prog Neurobiol*. 2001;63:71–124.
48. Canals JM, Pineda JR, Torres-Peraza JF, et al. Brain-derived neurotrophic factor regulates the onset and severity of motor dysfunction associated with enkephalinergic neuronal degeneration in Huntington's disease. *J Neurosci*. 2004;24:7727–7739.
49. Harada C, Harada T, Quah HM, et al. Role of neurotrophin-4/5 in neural cell death during retinal development and ischemic retinal injury in vivo. *Invest Ophthalmol Vis Sci*. 2005;46:669–673.
50. Meyerrose TE, Roberts M, Ohlemiller KK, et al. Lentiviral-transduced human mesenchymal stem cells persistently express therapeutic levels of enzyme in a xenotransplantation model of human disease. *Stem Cells*. 2008;26:1713–1722.
51. Machalinska A, Kawa M, Pius-Sadowska E, et al. Endogenous regeneration of damaged retinal pigment epithelium following low dose sodium iodate administration: an insight into the role of glial cells in retinal repair. *Exp Eye Res*. 2013;112:68–78.
52. Magabo KS, Horwitz J, Piatigorsky J, Kantorow M. Expression of betaB(2)-crystallin mRNA and protein in retina, brain, and testis. *Invest Ophthalmol Vis Sci*. 2000;41:3056–3060.
53. Nakata K, Crabb JW, Hollyfield JG. Crystallin distribution in Bruch's membrane-choroid complex from AMD and age-matched donor eyes. *Exp Eye Res*. 2005;80:821–826.
54. Basha E, O'Neill H, Vierling E. Small heat shock proteins and α-crystallins: dynamic proteins with flexible functions. *Trends Biochem Sci*. 2012;37:106–117.
55. Fort PE, Lampi KJ. New focus on alpha-crystallins in retinal neurodegenerative diseases. *Exp Eye Res*. 2011;92:98–103.
56. Xi J, Farjo R, Yoshida S, Kern TS, Swaroop A, Andley UP. A comprehensive analysis of the expression of crystallins in mouse retina. *Mol Vis*. 2003;9:410–419.
57. Liedtke T, Schwamborn JC, Schröer U, Thanos S. Elongation of axons during regeneration involves retinal crystallin beta b2 (crybb2). *Mol Cell Proteomics*. 2007;6:895–907.
58. Fischer D, Hauk TG, Müller A, Thanos S. Crystallins of the beta/gamma-superfamily mimic the effects of lens injury and promote axon regeneration. *Mol Cell Neurosci*. 2008;37:471–479.
59. Böhm MR, Melkonyan H, Oellers P, Thanos S. Effects of crystallin-β-b2 on stressed RPE in vitro and in vivo. *Graefes Arch Clin Exp Ophthalmol*. 2013;251:63–79.
60. Böhm MR, Pfrommer S, Chiwitt C, Brückner M, Melkonyan H, Thanos S. Crystallin-β-b2-overexpressing NPCs support the survival of injured retinal ganglion cells and photoreceptors in rats. *Invest Ophthalmol Vis Sci*. 2012;53:8265–8279.
61. Thanos S, Böhm MR, Schallenberg M, Oellers P. Traumatology of the optic nerve and contribution of crystallins to axonal regeneration. *Cell Tissue Res*. 2012;349:49–69.

ED: Please verify the accuracy of any edits made to the article summary below.

We show that MSCs transduced to express NT-4 are capable of long-term survival after intravitreal injection and delivery of NT-4 resulting in improvements of retinal function. We describe mechanisms underlying the protective effect and the signaling pathways supporting the survival of injured cells.

Investigative Ophthalmology & Visual Science